



## Evaluation of near-threshold fatigue crack propagation in Ti-6Al-4V Alloy with harmonic structure created by Mechanical Milling and Spark Plasma Sintering

S. Kikuchi, T. Imai, H. Kubozono, Y. Nakai

*Department of Mechanical Engineering, Kobe University, 1-1 Rokkodai, Nada, Kobe, 6578501, Japan*

*kikuchi@mech.kobe-u.ac.jp, 147t313t@stu.kobe-u.ac.jp, 159t323t@stu.kobe-u.ac.jp, nakai@mech.kobe-u.ac.jp*

A. Ueno, K. Ameyama

*Department of Mechanical Engineering, Ritsumeikan University*

*ueno01@fc.ritsumei.ac.jp, ameyama@st.ritsumei.ac.jp*

**ABSTRACT.** Titanium alloy (Ti-6Al-4V) having a bimodal “harmonic structure”, which consists of coarse-grained structure surrounded by a network structure of fine grains, was fabricated by mechanical milling (MM) and spark plasma sintering (SPS) to achieve high strength and good plasticity. The aim of this study is to investigate the near-threshold fatigue crack propagation in Ti-6Al-4V alloy with harmonic structure. Ti-6Al-4V alloy powders were mechanically milled in a planetary ball mill to create fine grains at powder’s surface and the MM-processed powders were consolidated by SPS. *K*-decreasing fatigue crack propagation tests were conducted using the DC(T) specimen (ASTM standard) with harmonic structure under the stress ratios, *R*, from 0.1 to 0.8 in ambient laboratory atmosphere. After testing, fracture surfaces were observed using scanning electron microscope (SEM), and crack profiles were analyzed using electron backscatter diffraction (EBSD) to discuss the mechanism of fatigue crack propagation. Threshold stress intensity range,  $\Delta K_{th}$ , of the material with harmonic structure decreased with stress ratio, *R*, whereas the effective stress intensity range,  $\Delta K_{eff}$ , showed constant value for *R* lower than 0.5. This result indicates that the influence of the stress ratio, *R*, on  $\Delta K_{th}$  of Ti-6Al-4V with harmonic structure can be concluded to be that on crack closure. Compared to the compact prepared from as-received powders with coarse acicular microstructure,  $\Delta K_{th}$  value of the material with harmonic structure was low. This was because the closure stress intensity,  $K_{cl}$ , in the material with harmonic structure was lower than that of the coarse-grained material due to the existence of fine grains. In addition, the effects of the grain size on the fatigue crack propagation behaviors of Ti-6Al-4V alloy were investigated for the bulk homogeneous material. The effects of the stress ratio and the grain size on the fatigue crack propagation of the material with harmonic structure were quantified.

**KEYWORDS.** Fatigue; Titanium alloy; Crack closure; Ultra-fine grain; Powder metallurgy; Harmonic structure.



## INTRODUCTION

**T**i-6Al-4V has been widely used for structural applications such as bio-implants and aerospace components due to its high specific strength and excellent corrosion resistance. Recently, improving mechanical properties of materials are required to increase structural reliability and reduce the size and weight of various components. Since mechanical properties of metallic materials are determined by their microstructural factors, the grain-refinement process is effective to improve their yield strength [1, 2] and fatigue strength. However, a homogeneous fine-grained structure generally leads to decrease the ductility of materials due to their plastic instability.

Previous investigations have reported the microstructural design which improves both of strength and ductility of materials [3-6]. Wang et al. [3] reported that pure copper with a bimodal grain size distribution created by a thermo-mechanical treatment exhibited stable tensile deformation leading to a high tensile ductility. The author's group [7-13] has developed an exquisite microstructural design, called "harmonic structure", which consists of coarse-grained structure surrounded by a network structure of fine grains. In the previous studies, metallic materials with harmonic structure, such as pure copper [7], stainless steel [8-10], Co-Cr-Mo alloy [11], commercially pure titanium [12] and Ti-6Al-4V alloy [13, 14] exhibited high strength and high ductility compared to their homogeneous counterparts. The authors have focused on the fatigue properties of the Ti-6Al-4V alloy with harmonic structure and reported that a fatigue crack was initiated from the coarse-grained structure in the harmonic structure in 4-points bending [14]. However, fatigue crack growth changes depending on the stress ratio and grain size of materials [15-17] so that the fatigue crack propagation of the material with a bimodal harmonic structure should be examined to achieve the practical use of it.

The present work deals with the evaluation of the near-threshold fatigue crack propagation of the Ti-6Al-4V alloy with a bimodal harmonic structure, which exhibits superior mechanical properties. Furthermore, the effects of the stress ratio and the grain size on the fatigue crack propagation of the material with harmonic structure were investigated on the basis of the crack closure concept, and its mechanism is discussed from viewpoints of fractography and crystallography.

## EXPERIMENTAL PROCEDURES

### Material

**T**he material used in the present study was a Ti-6Al-4V alloy with the chemical composition shown in Tab. 1. This Ti-6Al-4V powder (186  $\mu\text{m}$  diameter) was produced using the plasma rotating electrode process (PREP). The powders were mechanically milled (MM) in a Fritch P-5 planetary ball mill with tungsten carbide vial and SUJ2 steel balls in the argon gas atmosphere at room temperature. Mechanical milling was performed at a rotational speed of 200 rpm for 90 ks under the condition of the ball-to-powder mass ratio 1.8 : 1. After mechanical milling, the powders were consolidated by a spark plasma sintering (SPS) at 1123 K for 1.8 ks under vacuum and 50 MPa applied stress using a graphite die with 25 mm internal diameters (Harmonic series). In addition, the compact prepared from the as-received initial (IP) powders were also prepared as a coarse-grained material (IP series). The Harmonic series exhibits higher strength and ductility compared to the IP series as shown in Tab. 2 [13].

Fig. 1 shows the image quality (IQ) maps obtained by EBSD for the (a) IP and (b) Harmonic series [14]. The IP series has a coarse acicular microstructure, whereas the Harmonic series two different microstructures; fine-grained and coarse-grained structures. The fine-grained structure formed a network structure and the coarse-grained structure was surrounded by the fine-grained structure network. Minimum grain size in the Harmonic is about 1.1  $\mu\text{m}$  [13].

Al	V	Fe	H	N	O	C	Ti
6.51	4.26	0.17	0.0023	0.003	0.18	0.01	Bal.

Table 1: Chemical composition of Ti-6Al-4V alloy powder (mass%).

Microstructure	Yield strength, MPa	Ultimate tensile strength, MPa	Strain to fracture, %
IP series	802	864	20.9
Harmonic series	915	956	22.0

Table 2: Mechanical properties of the sintered compacts [13].

### Fatigue testing

The specimen used in the present study was the disk-shaped compact DC(T) specimen (2 mm thick, 25.2 mm wide). The sintered compacts (7.5 mm thickness, 25.2 mm wide) were cut to about 2.5 mm thickness and machined into the specimen. Then, specimen sides were polished with emery papers (#80 to #4000) and mirror-finished using SiO<sub>2</sub>. Fig. 2 shows the schematic illustration showing the specimen preparations.

Fatigue crack propagation tests were conducted in an electro-dynamic fatigue testing machine under the condition of five values of the stress ratio,  $R$ , ranging from 0.1 to 0.8. To approach the threshold,  $K$ -decreasing tests were conducted under the constant- $R$  loading regimen. Specimens were first fatigue pre-cracked for a minimum of 1 mm from the notch tip. The frequency of stress cycling was 30 Hz and the tests were carried out in ambient laboratory atmosphere. The value of the fatigue threshold,  $\Delta K_{th}$ , was defined as the maximum value under a crack growth rate of  $10^{-11}$  m/cycle. Crack lengths were monitored by unloading elastic compliance method [18]. The magnitude of crack closure was also monitored; closure stress intensity,  $K_{cl}$ , was obtained from the closure load,  $P_{cl}$ . Based on such measurements, an effective stress intensity range,  $\Delta K_{eff} = K_{max} - K_{cl}$ , was estimated. Where  $K_{max}$  is the maximum value of stress intensity factor.

### Microscopic observations

After testing, fracture surfaces were observed using scanning electron microscope (SEM) and crack profiles were observed and analyzed using electron backscatter diffraction (EBSD).

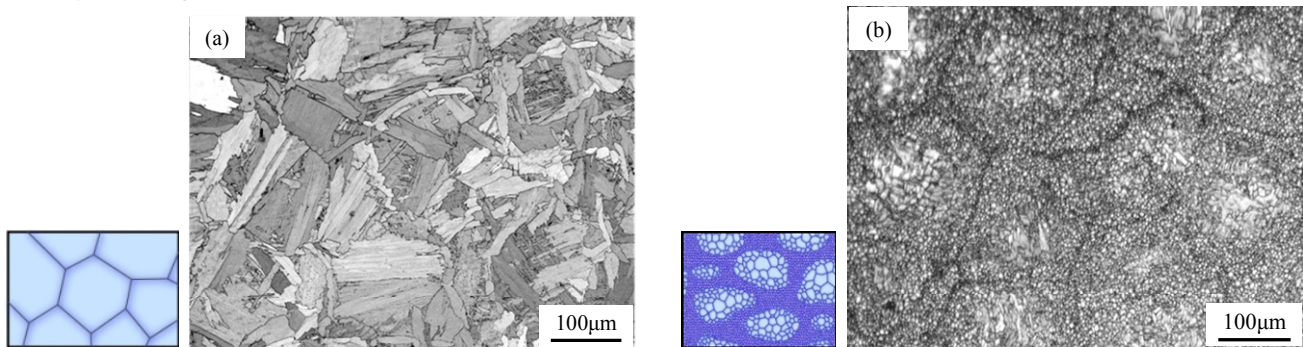


Figure 1: Image quality (IQ) maps obtained by EBSD for the (a) IP and (b) Harmonic series [14].

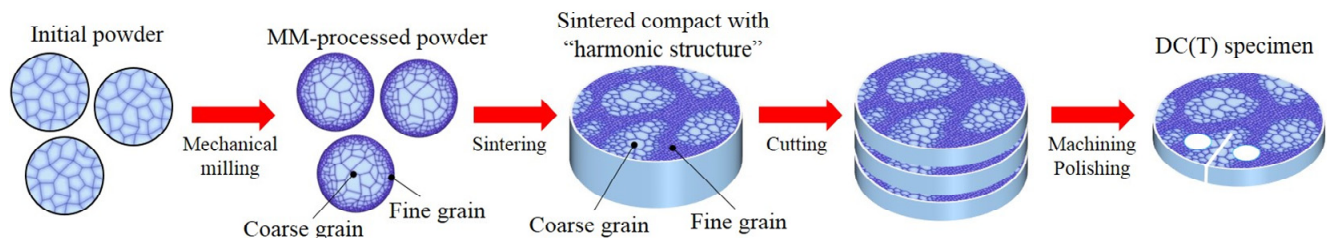


Figure 2: Schematic illustration showing the specimen preparations.

## RESULTS AND DISCUSSION

### Crack propagation behavior

The relation of the crack growth rate,  $da/dN$ , against the stress intensity range,  $\Delta K$ , is shown in Fig. 3 for the IP and Harmonic series. In each series, the threshold stress intensity range,  $\Delta K_{th}$ , decreased and crack growth rate,  $da/dN$ , increased at a given applied  $\Delta K$  value with increasing stress ratio,  $R$ . Furthermore, in the Harmonic series, crack growth rates were constantly higher at comparable  $\Delta K$  levels and thresholds were lower at comparable stress ratios compared to the IP series. Fig. 4 shows the relationship between  $\Delta K_{th}$  and  $R$  for each series. The value of  $\Delta K_{th}$  tended to be decreased approximately linearly with increasing  $R$  and the  $\Delta K_{th}$  value of the IP series was higher than that of the Harmonic series at comparable stress ratios. The relation between  $\Delta K_{th}$  and  $R$  in the IP and Harmonic series are expressed as Eqs. (1) and (2), respectively.



$$\Delta K_{th} = -2.60R + 4.39 \quad : \text{IP series} \tag{1}$$

$$\Delta K_{th} = -2.09R + 3.82 \quad : \text{Harmonic series} \tag{2}$$

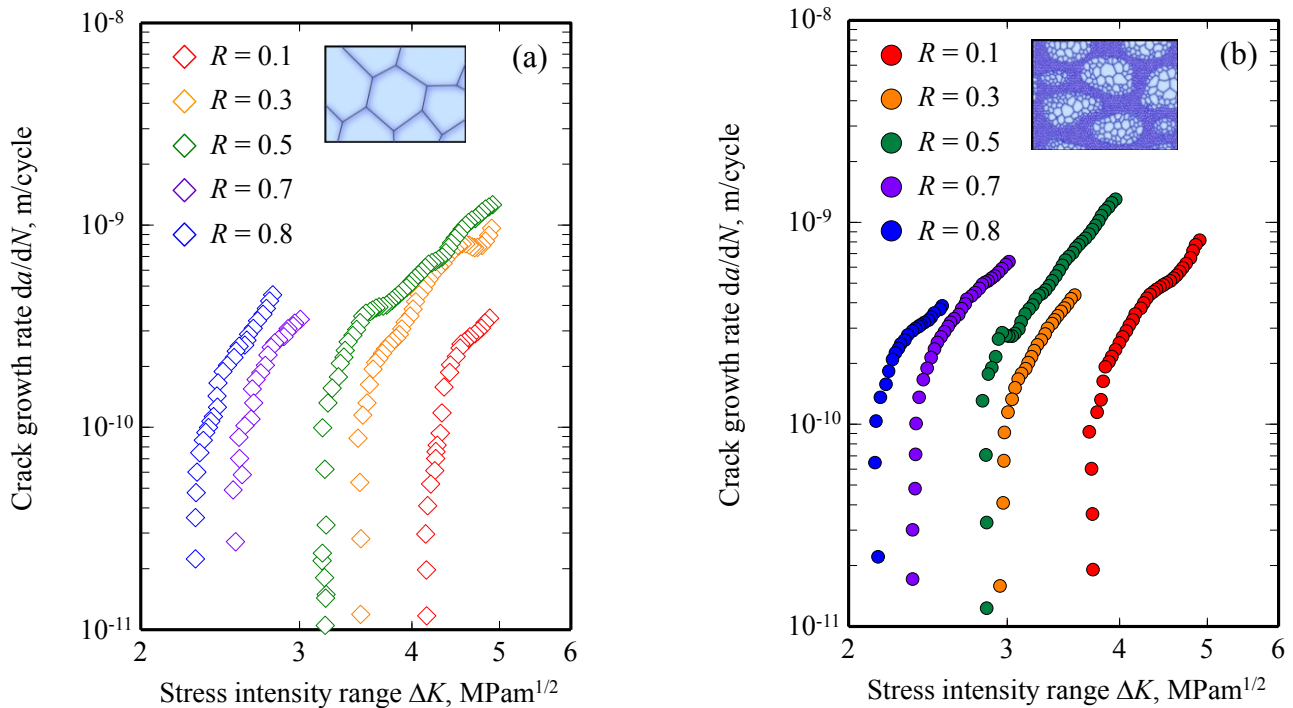


Figure 3: Relationship between crack growth rate and stress intensity range for the (a) IP and (b) Harmonic series.

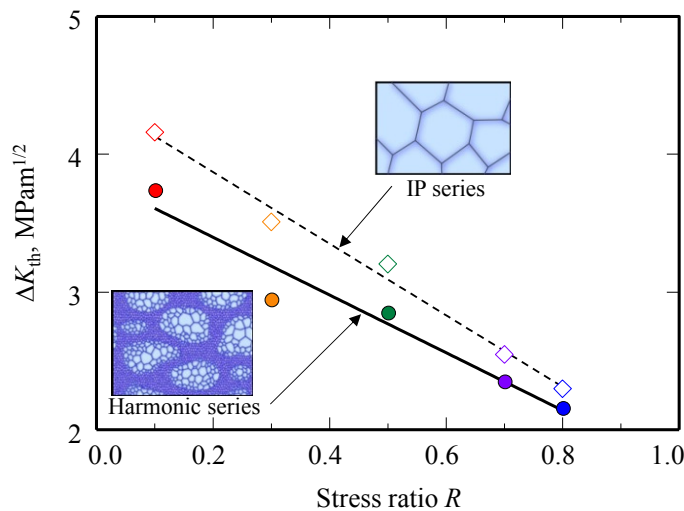


Figure 4: Relationship between threshold stress intensity range and stress ratio for the IP and Harmonic series.

### Crack closure

The role of stress ratio at near-threshold levels is generally attributed to crack closure [17]. Fig. 5 shows the relationship between  $da/dN$  and  $\Delta K_{eff}$ . In each series, the value of  $\Delta K_{eff}$  tended to normalize the stress ratio onto a single curve near threshold under  $R = 0.5$ . This result indicates that the effect of the stress ratio on the  $\Delta K_{th}$  disappears. However, when  $R$  is greater than 0.5,  $\Delta K_{th}$  value still decreased with increasing stress ratio,  $R$ . Same tendency was observed in the previous



study [16]. Ritchie et al. [16] has proposed the superposition model that the measured fatigue crack growth rate results from contributions from both mechanical fatigue cracking and sustain load cracking at high stress ratio. To examine the magnitude of crack closure, the ratio of closure stress intensity factor,  $K_{cl}$ , to maximum stress intensity factor,  $K_{max}$ , was calculated. Fig. 6 shows the relationship between  $K_{cl}/K_{max}$  and  $\Delta K_{eff}$  under various stress ratios. In this figure,  $K_{cl}/K_{max} = R$  when crack closure does not occur. At low stress ratios, the value of  $K_{cl}/K_{max}$  tended to be decreased with increasing  $\Delta K_{eff}$  and then was saturated to the constant value which is equal to stress ratio, whereas  $K_{cl}/K_{max}$  showed constant value independent of  $\Delta K_{eff}$  at high stress ratios. These results mean that crack closure occurs near the threshold at low stress ratios. Moreover, the  $K_{cl}/K_{max}$  value of the Harmonic series was lower than that of the IP series at low stress ratios (0.1, 0.3). Especially, at stress ratio of 0.5, crack closure occurred in the IP series, but the Harmonic series showed constant  $K_{cl}/K_{max}$  value. Consequently, the harmonic structure reduced the  $K_{cl}$  value of Ti-6Al-4V alloy, resulting in decreasing the value of  $\Delta K_{th}$ .

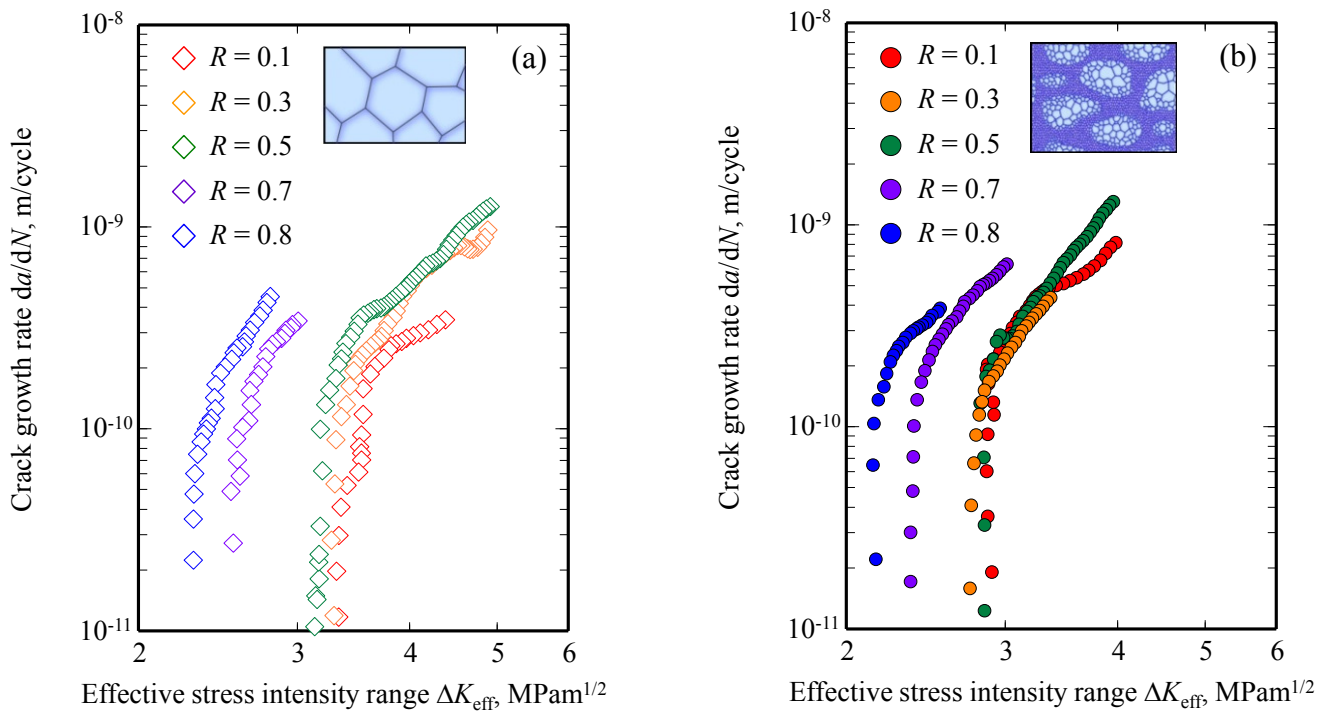


Figure 5: Relationship between crack propagation rate and effective stress intensity range for the (a) IP and (b) Harmonic series.

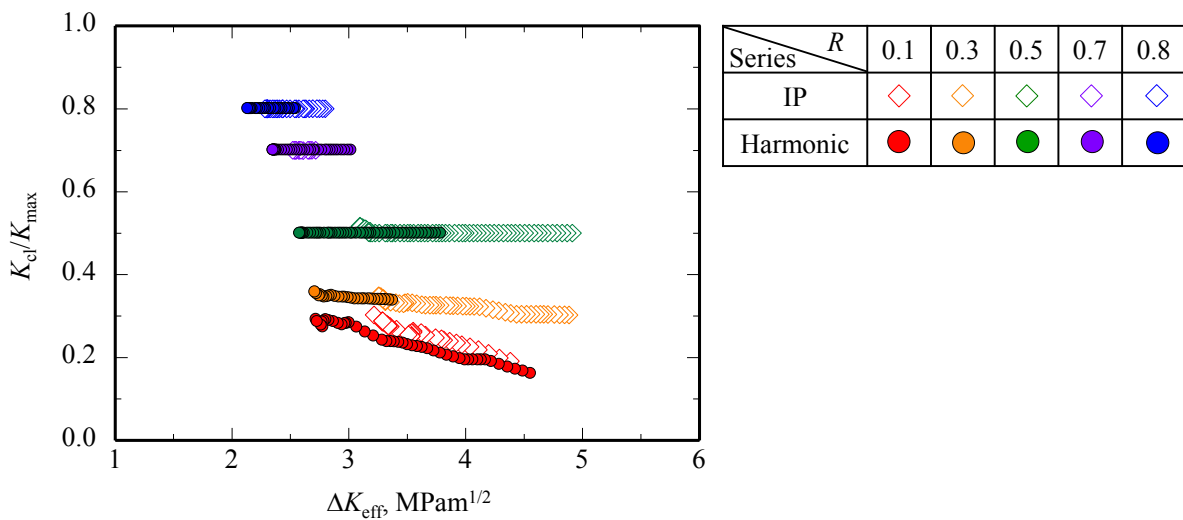


Figure 6: Relationship between  $K_{cl}/K_{max}$  and effective stress intensity range for the IP and Harmonic series.

### Effects of grain size on the fatigue crack propagation of Ti-6Al-4V alloy

To clarify the reason for decreasing  $\Delta K_{th}$  values of Ti-6Al-4V alloy by creating a harmonic structure as mentioned in the previous section, effects of grain size on the fatigue crack propagation were investigated for the bulk homogeneous material. Fig. 7 shows the relation of the crack growth rate,  $da/dN$  ( $R = 0.1$ ), against the stress intensity range,  $\Delta K$ , in the bulk homogeneous Ti-6Al-4V alloys with different grain size [19]. The  $\Delta K_{th}$  value of the coarse-grained bulk homogeneous material ( $d = 5.7 \mu\text{m}$ ) was high compared to the fine-grained one ( $d = 2.2 \mu\text{m}$ ). In contrast, as results of calculating the effective threshold stress intensity range,  $\Delta K_{eff,th}$ , the effect of grain size on the value of  $\Delta K_{th}$  disappears. The values of  $K_{cl}$  of the bulk homogeneous Ti-6Al-4V alloys are shown in Fig. 8. The  $K_{cl}$  value of the coarse-grained bulk material ( $d = 5.7 \mu\text{m}$ ) was higher than that of the fine-grained one ( $d = 2.2 \mu\text{m}$ ). In the case of the fine-grained material ( $d = 2.2 \mu\text{m}$ ), the value of  $K_{cl}$  decreased with increasing  $\Delta K$  and was saturated to approximately  $0.6 \text{ MPam}^{1/2}$ . The grain size strongly influences the behaviors of fatigue crack propagation and crack closure of Ti-6Al-4V alloy; the fine grains reduce the value of  $K_{cl}$ .

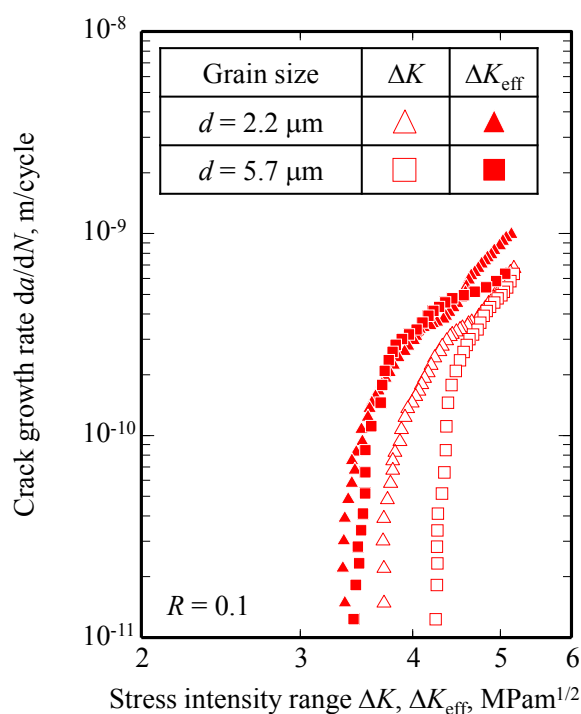


Figure 7: Relationship between crack growth rate and stress intensity range for the bulk specimen with homogeneous microstructure

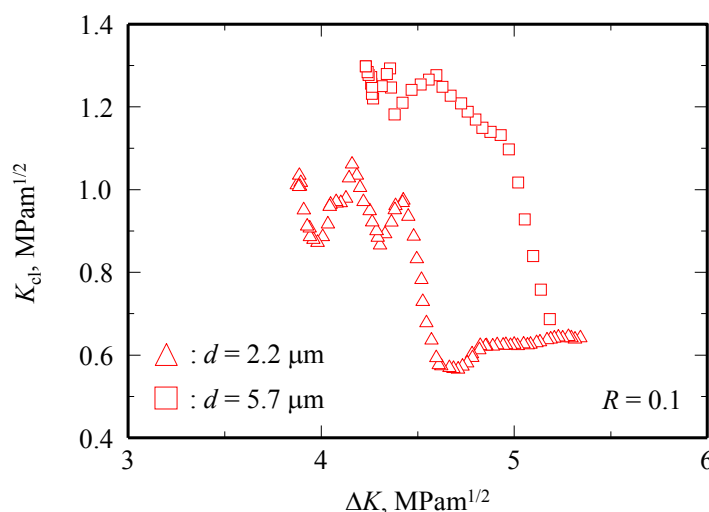


Figure 8: Relationship between crack closure intensity and stress intensity range for the bulk specimen with homogeneous microstructure.

### Fractography and crack profiles

The role of crack closure at near-threshold levels is generally attributed to the roughness-induced mechanism [20]. To characterize the surface topography of fracture surfaces, the three dimensional axonometric drawing was produced. Examples of axonometric drawings for the (a) IP and (b) Harmonic series are shown in Fig. 9. The surface topography of the IP series was rougher compared to the Harmonic series. Nalla et al. [15] has reported that the structure sensitivity of fatigue crack growth changes depending on the microstructure of Ti-6Al-4V alloy. Moreover, the coarser microstructure showed a more tortuous and deflected crack path than the finer microstructure, resulting in increasing the fatigue crack growth resistance due to the roughness-induced crack closure. The present study exhibited the same trend of the previous study [15].

Fig. 10 shows the inverse pole figure (IPF) maps obtained by EBSD at specimen's surface. In this figure, crack profiles are represented by black lines. In Fig. 10(a), crack profile of the Harmonic series showed very smooth and a fatigue crack was arrested at the coarse-grained structure, represented by the arrow mark. However, in some areas, a crack profile was influenced by the microstructure of the Harmonic series. Fig. 10(b) showed that a fatigue crack avoided propagating the coarse-grained structure of the Harmonic series, and propagated across the fine-grained structure.

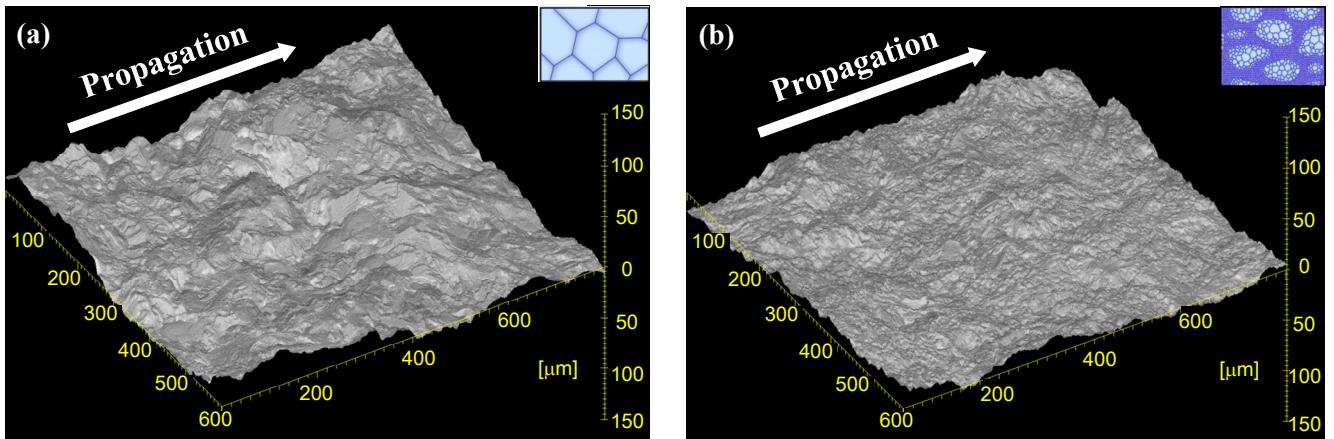


Figure 9: Axonometric drawing of fracture surfaces of the (a) IP and (b) Harmonic series ( $R = 0.1$ ).

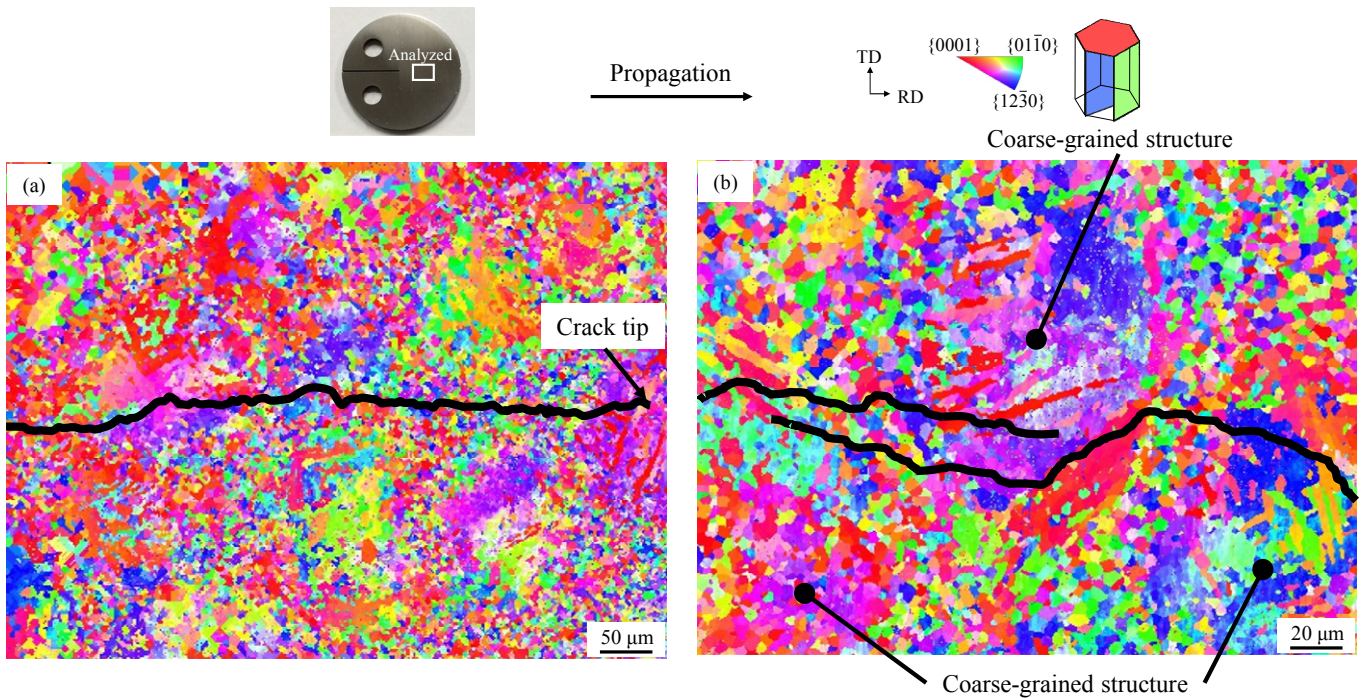


Figure 10: Inverse pole figure (IPF) maps of the crack profiles in the Harmonic series ((a)  $R = 0.1$  and (b)  $R = 0.5$ ).

*Estimation of the threshold stress intensity range of the material with harmonic structure*

Based on these results obtained in the present study, one might expect that a fine-grained structure in the harmonic structure dominates the fatigue crack propagation of the Harmonic series. To quantify the effects of fine-grained structure on the fatigue crack propagation of Ti-6Al-4V alloy, the threshold values of  $\Delta K$  obtained from the bulk homogeneous materials are re-plotted against the square root of the grain size,  $d$  in Fig. 11. For each  $R$  value, the value of  $\Delta K_{th}$  increased with square root of the grain size. The relation between  $\Delta K_{th}$  and  $d$  in the bulk homogeneous material are expressed as Eqs. (3) and (4), respectively.

$$\Delta K_{th} = 2.86 + 0.578d^{1/2} \quad : R = 0.1 \tag{3}$$

$$\Delta K_{th} = 2.61 + 0.259d^{1/2} \quad : R = 0.5 \tag{4}$$

where  $d$  is an average grain size of the bulk homogeneous material (m). The gradient obtained from the data of  $R = 0.1$  was higher than that of the  $R = 0.5$ . This result means that effect of grain size on the value of  $\Delta K_{th}$  is remarkable at low stress ratio.

Furthermore, the  $\Delta K_{th}$  value of the Harmonic series was estimated. Fig. 12 shows a schematic diagram explaining the estimation of threshold stress intensity range,  $\Delta K_{th}$ , of the Harmonic series based on the data of the bulk homogeneous materials. Assuming that the threshold stress intensity range decreases linearly with decreasing the square root of the grain size, we obtain the estimated  $\Delta K_{th}$  by substituting the grain size of fine-grained structure,  $d_{min}$ , of the Harmonic series into the Eqs. (3) and (4) for each  $R$ :

Estimated values of  $\Delta K_{th}$  of the Harmonic series are shown in Tab. 3. Comparing to values of  $\Delta K_{th}$  estimated and obtained by tests for each  $R$ , there were no obvious differences. This result indicates that the value of  $\Delta K_{th}$  of the Harmonic series can be estimated based on the fatigue crack propagation of the bulk homogeneous material and was determined by the crack propagation behavior of the fine-grained structure in the harmonic structure.

Consequently, a bimodal harmonic structure reduced the fatigue crack propagation resistance of Ti-6Al-4V alloy due to the existence of the fine-grained structure, which decreased the closure intensity factor,  $K_{cl}$ . However, there were little differences in  $\Delta K_{eff,th}$  values between the Harmonic series and the IP series so that additional mechanisms and factors may exist. This reason should be clarified in future works.

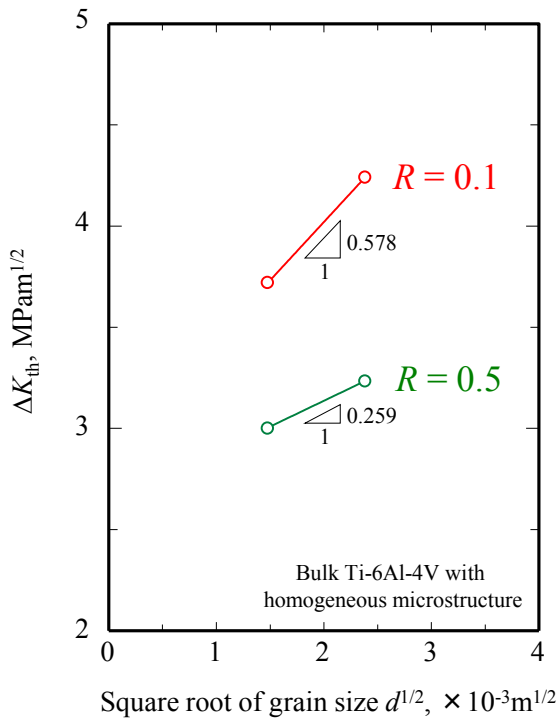


Figure 11: Relationship between threshold stress intensity range and grain size for the bulk specimen with homogeneous microstructure.

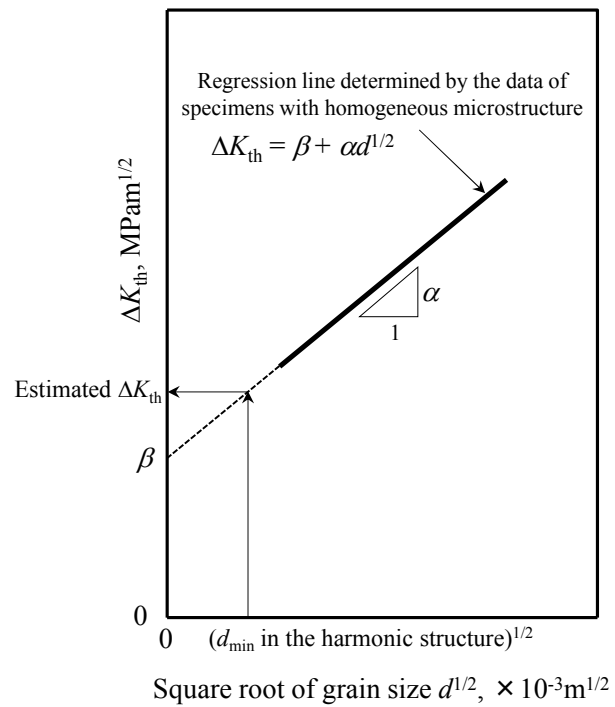


Figure 12: Schematic diagram explaining the estimation of threshold stress intensity range of the Harmonic series based on the data of the bulk specimen with homogeneous microstructure.

$\Delta K_{th}$ (MPam <sup>1/2</sup> )	$R = 0.1$	$R = 0.5$
Experimental	$3.62 \pm 0.16$ ( $n = 3$ )	$2.73 \pm 0.17$ ( $n = 2$ )
Estimated ( $d_{min} = 1.1 \mu\text{m}$ )	3.47	2.88

Table 3: Comparison of the values of  $\Delta K_{th}$  estimated and obtained by tests of the Harmonic series (Ave.  $\pm$  S.D.).





## CONCLUSIONS

In the present study, titanium alloy (Ti-6Al-4V) having a bimodal “harmonic structure”, which consists of coarse-grained structure surrounded by a network structure of fine grains, was fabricated by mechanical milling (MM) and spark plasma sintering (SPS), and its near-threshold fatigue crack propagation was investigated. The following conclusions were reached:

1. Threshold stress intensity range,  $\Delta K_{th}$ , of the material with harmonic structure decreases with increasing stress ratio,  $R$ , whereas the effective stress intensity range,  $\Delta K_{eff}$ , shows constant value for  $R$  lower than 0.5. The influence of the stress ratio,  $R$ , on  $\Delta K_{th}$  of Ti-6Al-4V with harmonic structure can be concluded to be that on crack closure.
2.  $\Delta K_{th}$  value of the material with harmonic structure is low compared to the compact prepared from as-received powders with coarse acicular microstructure due to the existence of the fine-grained structure. This is because the topography of fracture surfaces is smooth in the material with harmonic structure, which results in decreasing the closure stress intensity,  $K_{cl}$ .
3. A crack profile is influenced by the harmonic structure. The crack propagation behavior of the material with harmonic structure is determined by that of fine-grained structure in the harmonic structure.
4. The  $\Delta K_{th}$  value of the material with harmonic structure can be estimated based on the crack propagation behavior of the bulk homogeneous material.

## ACKNOWLEDGEMENT

The authors would like to acknowledge JSPS KAKENHI Grant Number 15K05677 and the Hattori Hokokai Foundation for the support.

## REFERENCES

- [1] Hall, E.O., The deformation and ageing of mild steel: III discussion of results, *Proc. Phys. Soc. B*, 64 (1951) 273–280.
- [2] Petch, N.J., The cleavage strength of polycrystals, *J. Iron and Steel Inst.*, 174 (1953) 25–28.
- [3] Wang, Y., Chen, M., Zhou, F., Ma, E., High tensile ductility in a nanostructured metal, *Nature*, 419 (2002) 912–915. DOI: 10.1038/nature01133
- [4] Fang, T.H., Li, W.L., Tao, N.R., Lu, K., Revealing extraordinary intrinsic tensile plasticity in gradient nano-grained copper, *Science*, 331 (2011) 1587–1590. DOI: 10.1126/science.1200177
- [5] Kim, C.P., Oh, Y.S., Lee, S., Kim N.J., Realization of high tensile ductility in a bulk metallic glass composite by the utilization of deformation-induced martensitic transformation, *Scripta Mater.*, 65 (2011) 304–307. DOI: 10.1016/j.scriptamat.2011.04.037
- [6] Kondoh, K., Nakanishi, N., Mimoto, T., Umeda, J., High strength and ductility mechanism of pure titanium materials with oxygen solid solution via powder metallurgy route, *Proc. 8th Int. Forum Adv. Mater. Sci. Tech.*, USB (2012) 3P-OS03-01.
- [7] Sawangrat, C., Kato, S., Orlov, D., Ameyama, K., Harmonic-structured copper: performance and proof of fabrication concept based on severe plastic deformation of powders, *J. Mater. Sci.*, 49 (2014) 6579–6585. DOI: 10.1007/s10853-014-8258-4
- [8] Ueno, A., Fujiwara, H., Rifai, M., Zhang, Z., Ameyama, K., Fractographical analysis on fracture mechanism of stainless steel having harmonic microstructure, *J. Soc. Mater. Sci., Jpn.*, 61 (2012) 686–691. DOI: 10.2472/jsms.61.686
- [9] Ciuca, O.P., Ota, M., Deng, S., Ameyama, K., Harmonic structure design of a SUS329J1 two phase stainless steel and its mechanical properties, *Mater. Trans.*, 54 (2013) 1629–1633. DOI: 10.2320/matertrans.MH201321
- [10] Zhang, Z., Vajpai, S.K., Orlov, D., Ameyama, K., Improvement of mechanical properties in SUS304L steel through the control of bimodal microstructure characteristics, *Mater. Sci. Eng. A*, 598 (2014) 106–113. DOI: 10.1016/j.msea.2014.01.023



- [11] Sawangrat, C., Yamaguchi, O., Vajpai, S.K., Ameyama, K., Application of harmonic structure design to biomedical Co–Cr–Mo alloy for improved mechanical properties, *Mater. Trans.*, 55 (2014) 99–105. DOI: 10.2320/matertrans.MA201303
- [12] Sekiguchi, T., Ono, K., Fujiwara, H., Ameyama, K., New microstructure design for commercially pure titanium with outstanding mechanical properties by mechanical milling and hot roll sintering, *Mater. Trans.*, 51 (2010) 39–45. DOI: 10.2320/matertrans.MB200913
- [13] Vajpai, S.K., Ota, M., Watanabe, T., Maeda, R., Sekiguchi, T., Kusaka, T., Ameyama, K., The development of high performance Ti-6Al-4V alloy by via a unique microstructure design with bimodal grain size distribution, *Metall. Mater. Trans. A*, 46 (2015) 903–914. DOI: 10.1007/s11661-014-2649-7
- [14] Kikuchi, S., Takemura, K., Hayami, Y., Ueno, A., Ameyama, K., Evaluation of the fatigue properties of Ti-6Al-4V alloy with harmonic structure in 4-points bending, *J. Soc. Mater. Sci., Jpn.*, 64 (2015) in press.
- [15] Nalla, R.K., Boyce, B.L., Campbell, J.P., Peters, J.O., Ritchie, R.O., Influence of microstructure on high-cycle fatigue of Ti-6Al-4V: bimodal vs. lamellar structures, *Metall. Mater. Trans. A*, 33 (2002) 899–918. DOI: 10.1007/s11661-002-1023-3.
- [16] Boyce, B.L., Ritchie, R.O., Effect of load ratio and maximum stress intensity on the fatigue threshold in Ti-6Al-4V, *Eng. Fract. Mech.*, 68 (2001) 129–147. DOI: 10.1016/S0013-7944(00)00099-0.
- [17] Nakai, Y., Tanaka, K., The effects of stress ratio and grain size on near-threshold fatigue crack propagation in low-carbon steel, *Eng. Fract. Mech.*, 15 (1981) 291–302. 10.1016/0013-7944(81)90062-X.
- [18] Kikukawa, M., Jono, M., Tanaka, K., Takatani, Measurement of fatigue crack propagation and crack closure at low stress intensity level by unloading elastic compliance method, *M., J. Soc. Mater. Sci., Jpn.*, 25 (1976) 899–903.
- [19] Nakamura, Y., Yoshida, S., Kikuchi, S., Ueno, A., Evaluation of the effects of low temperature nitriding on 4-points bending fatigue properties of Ti-6Al-4V alloy, *Proc. Asian-Pacific Conf. Fract. Strength 2014 and the Int. Conf. Struct. Integrity and Failure*, (2014) 93–98.
- [20] Ogawa, T., Tokaji, K., Ohya, K., The effect of microstructure and fracture surface roughness on fatigue crack propagation in a Ti-6Al-4V alloy, *Fatigue Fract. Eng. Mater. Struct.*, 16 (1993) 973–982. DOI: 10.1111/j.1460-2695.1993.tb00132.x